Comparison of the Mason and KLM Equivalent Circuits for Piezoelectric Resonators in the Thickness Mode

Stewart Sherrit, Sean P. Leary, and Yoseph Bar-Cohen
Jet Propulsion Laboratory, California Institute of Technology, Pasadena, CA

To be Submitted to the IEEE UFFC Transactions

Abstract – The parameters of the KLM and Mason's equivalent circuits in the thickness mode are derived to include dielectric, elastic and piezoelectric loss. The models are compared under various boundary conditions with and without acoustic layers to the analytical solutions of the wave equation. We show that in the case of a free resonator (short circuit on the acoustic ports) both Mason's circuit and the KLM model produce impedance data that is the exact equivalent of the data produced by the analytical solution. In the case where both piezoelectric surfaces are rigidly fixed, the analytical solution and Mason's circuit describe impedance data that is associated with the clamped capacitance C_O. The KLM circuit was shown to have infinite impedance at the electric port when the acoustics ports were open circuited. In the case where one of the piezoelectric surfaces is rigidly fixed the analytical solution and Mason's circuits describe an identical quarter wavelength resonator whereas the KLM circuit is shown to describe a half wave resonator under the same conditions. Similar discrepancies between the analytical solution and the KLM model are observed for acoustic elements with large acoustic impedance. It is interesting to note that in the case where acoustic layers had lower acoustic impedance than the piezoelectric material (low density/velocity or thin layers) the KLM model was found to approximate the analytical solution. These discrepancies between the KLM model and the analytical solutions are independent of loss and are also found in cases where loss-less resonators are modeled. The limitations discussed above are important to address due to the wide use of the KLM model. Therefore, we have determined an alternative equivalent circuit, which contains all the salient features of the KLM but is not limited to low acoustic impedance elements

I. INTRODUCTION

Analytical solutions to the wave equation in piezoelectric materials can be quite cumbersome to derive from first principles in all but a few cases. Mason[1],[2] was able to show that for one-dimensional analysis most of the difficulties in deriving the solutions could be overcome by borrowing from network theory. He presented an exact equivalent circuit that separated the piezoelectric material into an electrical port and two acoustic ports through the use of an ideal electromechanical transformer as shown in Figure 1b. The model has been widely used for free and mass loaded resonators[3], transient response[4], material constant determination[5], and a host of other applications[6]. One of the perceived problems with the model is that it required a negative capacitance at the electrical port. Although Redwood[4] showed that this capacitance could be transformed to the acoustic side of the transformer and treated like a length of the acoustic line it was still thought to be "un-physical". In an effort to remove circuit elements between the top of the transformer and the node of the acoustic transmission line Krimholtz, Leedom and Matthae[7] published an alternative equivalent circuit as shown in Figure 1c. The model is commonly referred to as the KLM model and has been used extensively in the medical imaging community in an effort to design high frequency transducers [8],[9], multilayers[10], and arrays[11]. To investigate the validity of these models under various boundary conditions a comparison was made between the exact analytical solution for a one-dimensional wave and the Mason and KLM equivalent circuits. Additional acoustic layers were also investigated.

II. DESCRIPTION OF THE MODELS

The KLM and Mason's model are shown in Figure 1 along with the free resonator equation of the thickness mode derived from the linear piezoelectric equations and the wave equation [3] which has been adopted by the IEEE Standard on Piezoelectricity[12] for determination of the thickness material constants.

The constants of each model are shown in Table 2. In the KLM and Mason's equivalent circuit an electrical port is connected to the center node of the two acoustic ports representing the front and back face of the transducer. On the electrical port of the transformer all circuit elements are standard electrical elements and the voltage is related to the current via V =ZI where Z is an electrical impedance. On the acoustical side of the transformer the force F and the velocity v are related through $F = Z_a v$ where Z_a is the specific acoustic impedance $Z_a \propto \rho v A$ where ρ is the density, v is the longitudinal velocity of the piezoelectric material and A is the area. It should be noted that the italic $v = \partial u/\partial t$ is a variable of the circuit model while the straight v is a constant of the material. The transformer is an ideal electromechanical transformer that conserves electrical and mechanical power during the transformation. A voltage V transformed to the acoustic port is found to equal a force $F = NV$ or $F = \phi V$ depending on the model used where N and ϕ are the turns ratio of the particular model. A current is found to equal a velocity v through $v = I/N$ or $v = I/\phi$. The electrical impedance is transformed to an acoustic impedance using $Z_a = ZN^2$ or $Z_a = Z\phi^2$. To transform specific acoustic impedance into electrical impedance on the electrical port one divides by the square of the turns ratio. These models allow for the calculation of the velocity and force on any surface in the transducer as well as the electrical impedance as seen from the electrical port. In an effort to reduce possible confusion we will use only the electrical impedance for the comparison of the models.

The relationship between the constants of the free resonator and the KLM and Mason's equivalent circuits are shown in Table 1. We treat the elastic, dielectric and piezoelectric constants of the free resonator as complex quantities as was outlined by Holland [13] and discussed by Berlincourt[14], Sittig [15], Katz[6], McSkimmin[17]. To calculate the circuit model constants to include losses proceed as in Table 2. For example using the complex material constants the circuit parameters Γ, N, ϕ, Z_0, M, C_0 are now all complex quantities. Identities for trigonometric functions with complex arguments can be found by expanding the trigonometric function in exponential form. A list of these identities can be found in earlier work on equivalent lumped circuit constants of free piezoelectric resonators [16].

III. Modeling

A. Open and Short Circuit Acoustic Ports

The KLM and Mason's equivalent circuits were compared under short circuit conditions. The material constants used are shown in Table 2 along with the equivalent circuit parameters of each mode. The impedance equations for the two models are shown in (1) and (2) below. Upon simplification it can be shown that these equations reduce to the equation for the free resonator shown in Table 1.

$$Z_m = Z_c \frac{\left[\left(Z_T/2 + Z_S\right)/N^2 - Z_C\right]}{\left(Z_T/2 + Z_S\right)/N^2} \tag{1}$$

$$Z_{klm} = Z_c + X_1 + \frac{Z_T/2}{\phi^2} \tag{2}$$

where $Z_c = 1/i\omega C_0$. Impedance data for the free resonator, Mason's equivalent circuit and the KLM circuit are shown in Figure 2. The data are identical and the curves overlap. Under short circuit conditions therefore both of these models describe the thickness extensional impedance resonance and either of these circuits or the equation for the free impedance resonator can be used to determine material properties.

The models were tested under the condition where one acoustic port was open circuited (rigidly fixed) and the other short-circuited (free to expand). The analytical solution is found in the same manner as is done for the free resonator except now instead of stress free boundary conditions (T(x=0)=T(x=t)=0) we have mixed boundary conditions (T(x=0)=0 and S (x=t)=0). Using these boundary conditions the analytical solution for this resonator geometry is

$$\mathbf{Z} = \frac{l}{i\omega A \varepsilon_{33}^{S}} \left(1 - \frac{\mathbf{k}_i^2 \tan\left(t\omega \sqrt{\frac{\rho}{\mathbf{c}_{33}^{D}}} \right)}{t\omega \sqrt{\frac{\rho}{\mathbf{c}_{33}^{D}}}} \right) \tag{3}$$

which is similar to the free resonator equation except for a factor of 2 in the argument and divisor of the tan function. The equations for Mason's equivalent circuit and the KLM equivalent circuit for these boundary conditions are.

$$Z_m = Z_c \frac{\left[(Z_T + Z_s)/N^2 - Z_C \right]}{(Z_T + Z_s)/N^2} \tag{4}$$

$$Z_{klm} = Z_c + X_1 + \frac{Z_T}{\phi^2} \tag{5}$$

The impedance data for all three models (equation (3) to (5)) is shown in Figure 3. The data was generated using the constants shown in Table 2. The analytical solution is found to overlap the

results from Mason's model. Both show a resonance at $t\omega/v^D = \pi/2$ which shows that at resonance the thickness $t=\lambda/4$ and the sample resonates as a quarter wavelength resonator. The resonance frequency of the KLM model remained unchanged and resonated as a half wavelength resonator ($t=\lambda/2$).

The discrepancies between the KLM and Mason's model are even more apparent in the case of a piezoelectric material rigidly fixed at both ends. Both the linear equations of piezoelectricity and Mason's model indicate that the impedance across the electrical port would be $Z = 1/i\omega C_0$ (the impedance due to the clamped static capacitance of the material). In the KLM model the impedance is found to be infinite across the electrical port.

B. Acoustic Elements

The results of the proceeding section suggest it would be informative to investigate the impedance of the two models in the case where layer/s are added to the thickness resonator. In order to accomplish this we use the network representation of a non-piezoelectric solid acoustic element as described by Redwood[4] and McSkimmin[17]. This network representation is shown in Figure 4. Like Mason's model this representation is the solution to the one-dimensional wave equation with open boundary conditions. In order to emphasize the versatility of this representation we have investigated the response of this network in the low and high frequency regimes when the front face of the layer is acoustically short circuited (free to expand) and open circuited (rigidly clamped). The back surface is driven by a sinusoidal force $F=F_o\cos(\omega t)$. For harmonic sinusoidal excitation in a linear system the displacement u_1 of the back face is related to the velocity v_1 by $v_1=i\omega u_1$. The acoustic impedance of the layer under open and short circuit conditions is

$$Z_{Open} = Z_T + Z_S \tag{6}$$

$$Z_{Short} = Z_T + \frac{Z_T Z_S}{Z_T + Z_S} \tag{7}$$

1) At high frequencies the acoustic element goes into resonance. The elastic properties, geometry and boundary conditions determine the resonance frequency. In the case where one face of the element is rigidly fixed (open circuit) the resonance frequency in determined from the minimum of Z_{Open} and the plate is found to resonate at $\lambda/4$. When the acoustic port is short-circuited the element is found to resonate at $\lambda/2$. The frequency response (derived from equations 6 and 7) of the logarithm of the velocity v is shown in Figure 5 for both the open and short circuit acoustic ports. The constants used for this simulation are shown in the figure caption

2) In the low frequency limit as $\omega \rightarrow 0$ the tan function $\tan(\omega L/2v) \rightarrow \omega L/2v$ while the $\sin(\omega L/v) \rightarrow \omega L/v$. The acoustic impedance of each element reduces to $Z_T \rightarrow i\rho A\omega L/2 = im\omega/2$, $Z_S \rightarrow \rho A v^2/i\omega L = Ac_{33}/i\omega L$ where m is the mass of the layer and c_{33} is the elastic stiffness. In the case where the front surface is rigidly fixed we note that at low frequencies $Z_S >> Z_T$

$$Z_{Open} = Z_S = Ac_{33}/i\omega L \tag{8}$$

and the total impedance appears capacitive with a capacitance $C = L/Ac_{33}$. The strain $S = u_1/L$ for a sinusoidal force $F_1 = F_0\cos(\omega t)$ is therefore

$$S = \frac{u_1}{L} = \frac{F}{i\omega L Z_{Open}} = -\frac{1}{c_{33}}\frac{F_0}{A}\cos(\omega t) \tag{9}$$

This is the equation of an elastic solid being strained (Hooke's Law) by the application of a sinusoidal force, which is exactly what one would expect.

In the case where the layer is short-circuited the total impedance at low frequency is

$$Z_{Short} = 2Z_T = im\omega \tag{10}$$

and the impedance is inductive with an inductance L = m the mass of the acoustic layer. The displacements of the front and back face u_1, u_2 are found to be

$$u_2 = u_1 = -\frac{1}{m}\frac{F_0}{\omega^2}\cos(\omega t) \tag{11}$$

which is the equation for a displacement of a mass driven by a harmonic force.

C. Layered Transducer Modeling

The analytical solution for the impedance of a piezoelectric film on a substrate derived from the wave equation was determined by Lakin, Kline and McCarron[18], A more recent derivation by Lukacs et al[19] extended the solution to include loss in the elastic, dielectric and piezoelectric constants and first order dispersion in the dielectric constant. The solution is valid for all cases where the lateral dimensions of the acoustic layer and the piezoelectric layer are much larger than either layer thickness. In the following section we compare the Mason's and KLM equivalent circuits to the analytical solution for a high impedance backing (stainless steel) and a low impedance backing (epoxy) to investigate the effects of including an acoustic layer on the various models. The models are similar to the models presented in Figure 1 however each model also has an acoustic element (ie. backing layer) as shown in Figure 4 on one of the acoustic ports

$$Z_m = Z_c \frac{\left[(Z_A + Z_S)/N^2 - Z_C\right]}{(Z_A + Z_S)/N^2} \tag{12}$$

$$Z_{klm} = Z_c + X_1 + \frac{Z_A}{\phi^2} \tag{13}$$

where Z_A is

$$Z_A = \frac{Z_T\left(Z_T + Z_T^B + \dfrac{Z_T^B Z_S^B}{Z_T^B + Z_S^B}\right)}{2Z_T + Z_T^B + \dfrac{Z_T^B Z_S^B}{Z_T^B + Z_S^B}} \tag{14}$$

The functions Z_T and Z_S are the acoustic elements of the piezoelectric defined in Figure 1 and Table 1. The functions $Z^B{}_T$ and $Z^B{}_S$ are the acoustic elements (sin and tan functions) of the backing layer shown in Figure 4. The superscript B is used to differentiate the backing layer impedance elements from the piezoelectric acoustic element in equation 14. The geometry stiffness, density and velocity, of the each of the backing layers are listed in Table 3. The piezoelectric properties used in this simulation are shown in Table 2.

The results for the epoxy backed transducer are shown in Figure 6. The analytical solution and the results from Mason's equivalent circuit are identical and overlap. The data from the KLM model has similar features to the other curves however the KLM data appears to have a higher mechanical Q and the major resonance is seen to occur at a slightly higher frequency. At low frequencies the data from the KLM model and the Mason's equivalent circuit begin to overlap.

The analytical solution, Mason's model and the KLM equivalent circuit data are shown in Figure 7 for the case where the piezoelectric is backed with stainless steel. The analytical soloution and Mason's model overlap over the entire spectra. The parallel resonance frequency

shifts down to $\approx \lambda/4$ in the data determined from the analytical soloution and Mason's equivalent circuit while the parallel resonance frequency of the KLM model is found to be considerably higher. These results suggest that caution should be exercised when using the KLM equivalent circuit to model high specific impedance acoustic elements in the transmission line.

IV. DISCUSSION

The proceeding results suggest that a problem exists when high impedance acoustic elements are included in the KLM model. Closer examination of the circuit models shown in Figure 1 indicates that the source of the problem is that the KLM model is only identical to the Mason's equivalent circuit when the acoustic ports are short-circuited at the piezoelectric surface. This can be shown by noting that one can not transform the parallel capacitance in the Mason's equivalent circuit to a series capacitance as found in the KLM model without knowing the full acoustic load. As well the turns ratio in the KLM model is only physical when the acoustic ports on the piezoelectric surfaces are shorted. The turns ratio used by Mason's comes directly from the linear equations of piezoelectricity and relate voltage to force and current to velocity. The turns ratio therefore is a constant and should have no frequency dependence.

These results suggest that there are limits to the applicability of the KLM model when acoustic layers are used. As a general rule it can be shown that the sum of the acoustic impedances on the front or back face due to additional acoustic elements must be less than $Z_T = i\rho v A\tan(\omega L/2v)$ of the piezoelectric material at the frequency of interest in order to accurately model the transducer. The reasons for the successes of the KLM equivalent circuit in modeling response, bandwidth, insertion loss, etc. appears to be due to the fact that the model is typically

used with low acoustic impedance elements (acoustic impedance is much lower than acoustic impedance of the piezoelectric material). As well the transducer model uses a real load for the water, which is much smaller than the acoustic impedance of the piezoelectric.

This means that at least one of the acoustic ports is almost a short. In Figure 8 we plot the electrical impedance of the KLM and Mason's model for the epoxy resonator shown in Figure 6 with a load impedance on the front face of $R_L = \rho v A = 265$ Rayls m^2. We have used $\rho = 1000$ kg/m^3 and $v = 1500$ m/s. to model transmission into water. The area A is the transducer area. As can be seen from the figure the baselines of the impedance data away from resonance overlap. The resonance of the KLM model is seen to occur at a slightly higher frequency and has a much sharper resonance than that of Mason's Model. It is worth noting that if the mechanical Q of the piezoelectric material is reduced by a factor of 2 when calculating the KLM parameters the impedance of the KLM and Mason's equivalent circuits are almost identical. This means that an inaccurate evaluation of the mechanical Q of the piezoelectric material can compensate for the approximations used in the KLM model. It should be noted that although one can determine a good fit to the data using the KLM model in this case the model looses some of it predictive properties due to the adjustments to the Q of the piezoelectric material.

Due to the widespread use of the KLM model and the limitations that we have discussed above we have determined an alternative equivalent circuit which contains all the salient features of the KLM however it is not limited to low acoustic impedance elements. The model is shown in Figure 9. In series on the electrical side of the transducer there is a clamped capacitance and a reactance that is a function of the clamped capacitance and the acoustic elements. An acoustic transmission line is on the acoustic side of the transformer and like the KLM model the leads

from the transformer are shorted to the center of the transmission line. The elements of the model are:

$$\mathbf{N} = \mathbf{C}_0 h_{33} \tag{15}$$

$$\mathbf{C}_0 = \frac{\varepsilon_{33}^S A}{t} \tag{16}$$

$$\mathbf{Z}_C = \frac{1}{i\omega \mathbf{C}_0} \tag{17}$$

$$\mathbf{Z}_\mathbf{R} = \frac{(\mathbf{Z}_T + \mathbf{Z}_F)(\mathbf{Z}_T + \mathbf{Z}_B)}{(2\mathbf{Z}_T + \mathbf{Z}_F + \mathbf{Z}_B)} \tag{18}$$

$$\mathbf{Z}_T = i\mathbf{Z}_0 \tan(\Gamma t/2) \tag{19}$$

$$\mathbf{Z}_S = -i\mathbf{Z}_0 \csc(\Gamma t) \tag{20}$$

$$Z_0 = \rho A v^D = A\sqrt{\rho\, \mathbf{c}_{33}^D} \tag{21}$$

$$\Gamma = \frac{\omega}{v^D} = \omega\sqrt{\frac{\rho}{c_{33}^D}} \tag{22}$$

$$\mathbf{X}_0 = -\frac{\left(\mathbf{N}^2\mathbf{Z}_C^2 + \mathbf{Z}_R\mathbf{Z}_S/\mathbf{N}^2 + \mathbf{Z}_R^2\right)}{\mathbf{Z}_S + \mathbf{Z}_R} = \frac{-\left(\mathbf{N}^2\mathbf{Z}_C^2\right)}{\mathbf{Z}_S + \mathbf{Z}_R} - \frac{\mathbf{Z}_R}{\mathbf{N}^2} \tag{23}$$

Where $\mathbf{Z}_F$ and $\mathbf{Z}_B$ are the sum of acoustic elements on the front and back face of the piezoelectric material. $\mathbf{Z}_R$ is the resultant of the parallel combination of the sum of acoustic impedance elements of the front and back faces of the piezoelectric and any attached layers The electrical impedance of the transducer as seen across the piezoelectric electrical ports is

$$\mathbf{Z} = \mathbf{Z}_C + \mathbf{X}_0 + \frac{\mathbf{Z}_R}{N^2} \tag{24}$$

The model has been tested and found to reproduce data generated by Mason's model for the open and short acoustic ports as well as for the stainless steel and epoxy backed resonators.

IV. CONCLUSIONS

The parameters of the KLM and Mason's equivalent circuits in the thickness mode were derived to include dielectric, elastic and piezoelectric loss. The models were compared under various boundary conditions with and without acoustic layers to the analytical solutions to the wave equation. It was shown that in the case of a free resonator (short circuit on the acoustic ports) both Mason's circuit and the KLM model produce impedance data that is the exact equivalent of the data produced by the analytical solution. While in the case where both piezoelectric surfaces are rigidly fixed the analytical solution and Mason's circuit describes impedance data that is associated with the clamped capacitance C_O. The KLM circuit was shown to have infinite impedance at the electric port when the acoustics ports were open circuited. When one of the piezoelectric surfaces is rigidly fixed the analytical solution and Mason's circuits describe an identical quarter wavelength resonator whereas the KLM circuit is shown to describe a half wave resonator under the same conditions. Similar discrepancies between the analytical solution and the KLM model for acoustic elements with large acoustic impedance were discussed. It is interesting to note that when the acoustic layers had lower acoustic impedance than the piezoelectric material (low density/velocity or thin layers) the KLM model approximates the analytical solution. These discrepancies between the KLM model and the analytical solutions findings were determined to be are independent of loss and they hold for the loss-less resonators. The limitations discussed above are important to address due the wide use of the KLM model. Therefore, we have determined an alternative equivalent circuit, which contains all the salient features of the KLM but is not limited to low acoustic impedance elements

ACKNOWLEDGMENT

The research at the Jet Propulsion Laboratory (JPL), a division of the California Institute of Technology, was carried out under a contract with the National Aeronautics Space Agency (NASA).

REFERENCES

[1] W..P. Mason, Electromechanical Transducers and Wave Filters, Princeton, NJ, Van Nostrand, 1948
[2] W.P. Mason, Physical Acoustics and the Properties of Solids, D. Van Nostrand Co., Princeton, NJ, 1958
[3]D. A. Berlincourt, D.R. Curran, H. Jaffe, "Chapter 3- Piezoelectric and Piezomagnetic Material and their Function in Transducers, pp. 169-270, Physical Acoustics-*Principles and Methods*, Volume 1-Part A, ed. W.P. Mason Academic Press, New York, 1964
[4] M. Redwood, "Transient Performance of a Piezoelectric Transducer", Journal of the Acoustical Society of America, **33**, pp.527-536, 1961
[5] S. Saitoh, H Honda, N. Kaneko, M. Izumi, S. Suzuki, The Method of Determining k_t and Q_m for low Q piezoelectric materials" Proceedings of the IEEE Symposium on Ultrasonics, San Francisco, CA, pp. 620-623, 1985
[6] Solid State Magnetic and Dielectric Devices, edited by H.W. Katz, John Wiley and Sons, New York , 1959
[7] R. Krimholtz, D.A. Leedom, G.L. Matthaei, "New Equivalent Circuit for Elementary Piezoelectric Transducers", Electron Letters, Electron. Lett. **6**, pp. 398-399,1970
[8] M. J. Zipparo, K.K. Shung, T.S. Shrout, "Piezoceramics for High Frequency (20-100 MHz) Single Element Imaging Transducers", IEEE Trans on Ultrasonics, Ferroelectrics and Frequency Control, **44**, pp.1038-1048, 1997
[9] F.S. Foster, L.K. Ryan, D.H. Turnbull, "Characterization of Lead Zirconate Titanate Ceramics for Use in Miniature High Frequency (20-80 MHz) Transducers, IEEE Trans on Ultrasonics, Ferroelectrics and Frequency Control , **38**, pp. 446-453, 1991
[10] Q. Zhang, P.A. Lewin, P.E. Bloomfield, "PVDF Transducers- A Performance Comparison of Single-Layer and Multilayer Structures", IEEE Trans on Ultrasonics, Ferroelectrics and Frequency Control, **44**, pp.1148-1156, 1997
[11] R.L. Goldberg, M.J. Jurgens, D.M. Mills, C.S. Henriquez, D.Vaughan, S. W. Smith, "Modeling of Piezoelectric Multilayer Ceramics Using Finite Element Analysis", IEEE Trans on Ultrasonics, Ferroelectrics and Frequency Control., **44**, pp. 1204-1214, 1997
[12] IEEE Standard on Piezoelectricity, IEEE/ANSI Std. 176-1987

[13]R. Holland, IEEE Transactions on Sonics and Ultrasonics, " Representations of the Dielectric, Elastic, and Piezoelectric Losses by Complex Coefficients", IEEE Transactions on Sonics and Ultrasonics, **SU-14**, pp.18-20, 1967

[14] D. A. Berlincourt, Chapter 2 -"Piezoelectric Crystals and Ceramics", Ultrasonic Transducer Materials, edited by O.E. Mattiat, Plenum Press, New York, 1971

[15]E.K. Sittig, Chapter 5-, "Design and Technology of Piezoelectric Transducers for Frequencies above 100 MHz", Physical Acoustics, Vol IX, edited by W.P. Mason, R.N. Thurston, Academic Press, New York, 1972

[16] S. Sherrit, H.D. Wiederick, B.K. Mukherjee, M. Sayer, "An accurate equivalent circuit for the unloaded piezoelectric vibrator in the thickness modes." J. Phys. D. (Applied Physics), **30**, pp. 2354-2363, 1997

[17] H.J. McSkimmin , "Chapter 4- Ultrasonic Methods for Measuring the Mechanical Properties of Liquids and Solids, pp. 271-334, Physical Acoustics-*Principles and Methods*, Volume 1-Part A, ed. W.P. Mason Academic Press, New York, 1964

[18] Kenneth M. Lakin, Gerald R. Kline, Kevin T. McCarron, "High Q Microwave Acoustic Resonators and Filters" IEEE Trans. On Microwave Theory and Techniques, **41**, pp. 2139-2146, 1993

[19] M. Lukacs, T. Olding, M. Sayer, R. Tasker, S. Sherrit, "Thickness mode material constants of a supported piezoelectric film", J. of Applied Physics , **85**, pp.2835-2843, 1999

List of Tables

List of Figures

Table 1. Sherrit et. al.

Free Resonator
$$\mathbf{Z} = \frac{l}{i\omega A \varepsilon_{33}^{S}}\left(1 - \frac{\mathbf{k}_t^2 \tan\left(\frac{t\omega}{2}\sqrt{\frac{\rho}{\mathbf{c}_{33}^{D}}}\right)}{\frac{t\omega}{2}\sqrt{\frac{\rho}{\mathbf{c}_{33}^{D}}}}\right)$$
ε_{33}^{S} clamped complex permittivity
$\mathbf{c}_{33}^{D}$ open circuit complex elastic stiffness
$\boldsymbol{k}_t$ complex electromechanical coupling
$\boldsymbol{k}_t^2 = \boldsymbol{e}_{33}^2 / \mathbf{c}_{33}^{D}\varepsilon_{33}^{S} = \boldsymbol{h}_{33}^2 \varepsilon_{33}^{S} / \mathbf{c}_{33}^{D}$
$\boldsymbol{h}_{33} = \boldsymbol{k}_t \sqrt{\mathbf{c}_{33}^{D} / \varepsilon_{33}^{S}}$
Mason's Model
$\mathbf{C}_0 = \frac{\varepsilon_{33}^{S} A}{t}$ $\quad$ $\mathbf{N} = \mathbf{C}_0 \boldsymbol{h}_{33}$
$\boldsymbol{Z}_0 = \rho\, A \boldsymbol{v}^D = A\sqrt{\rho\, \mathbf{c}_{33}^{D}}$ $\quad$ $\Gamma = \frac{\omega}{\boldsymbol{v}^D} = \omega\sqrt{\frac{\rho}{\boldsymbol{c}_{33}^{D}}}$
$Z_T = i\mathbf{Z}_0 \tan(\Gamma t/2)$ $\quad$ $Z_S = -i\mathbf{Z}_0 \csc(\Gamma t)$
KLM Model
$\mathbf{C}_0 = \frac{\varepsilon_{33}^{S} A}{t}$
$\boldsymbol{Z}_0 = \rho\, A \boldsymbol{v}^D = A\sqrt{\rho\, \mathbf{c}_{33}^{D}}$ $\quad$ $\mathbf{M} = \frac{\boldsymbol{h}_{33}}{\omega\, \boldsymbol{Z}_0}$
$\Gamma = \frac{\omega}{\boldsymbol{v}^D} = \omega\sqrt{\frac{\rho}{\boldsymbol{c}_{33}^{D}}}$ $\quad$ $X_1 = i\mathbf{Z}_0\mathbf{M}^2 \sin(\Gamma t/2)$
$Z_T = i\mathbf{Z}_0 \tan(\Gamma t/2)$ $\quad$ $\phi = \frac{1}{2\mathbf{M}} \csc(\Gamma t/2)$

Table 2. Sherrit et. al.

Material Constants and Geometry of Piezoelectric Material (Motorola 3203HD)		
$\rho = 7800$ kg/m^3	t = 0.001 m	Diameter = 0.015 m

$$\mathbf{c}_{33}^{D} \text{ (x } 10^{11} \text{ N/m}^2) = 1.77 \text{ (1 + 0.023i)}$$
$$\varepsilon_{33}^{S} \text{ (x } 10^{-8} \text{ F/m)} = 1.06 \text{ (1 - 0.053i)}$$
$$\boldsymbol{h}_{33} \text{ (x } 10^{9} \text{ V/m)} = 2.19 \text{ (1 + 0.029i)}$$
$$\boldsymbol{k}_t = 0.536 \text{ (1 - 0.0093i)}$$
$$\mathbf{C}_0 \text{ (nF)} = 1.87 \text{ (1 – 0.053i)}$$
$$\mathbf{N} \text{ (C/m)} = 4.11 \text{ (1 + 0.10i)}$$
$$\boldsymbol{v}_D \text{ (m/s)} = 4674 \text{ (1 + 0.012i)}$$
$$\Gamma/\omega \text{ (x}10^{-4} \text{ s/m)} = 2.10 \text{ (1 – 0.012i)}$$
$$\mathbf{M}\omega \text{ (x}10^{5} \text{ Vs/mkg)} = 3.33 \text{ (1 + 0.017i)}$$

Table 3. Sherrit et. al.

Material Constants and Geometry of the backing materials	
t = 0.001 m	Diameter = 0.015 m
Epoxy	Stainless Steel
ρ(kg/m^3) = 1100	ρ(kg/m^3) = 7890
$\mathbf{c}_{33}^{D}$ (x 10^9 N/m^2) = 5.3 (1 + 0.1i)	$\mathbf{c}_{33}^{D}$ (x 10^{11} N/m^2) = 2.645 (1 + 0.002i)
$\boldsymbol{v}_D$ (m/s) = 2200 (1 + 0.05i)	$\boldsymbol{v}_D$ (m/s) = 5790 (1 + 0.001i)
Γ/ω (x10^{-4} s/m) = 4.53 (1 – 0.05i)	Γ/ω (x10^{-4} s/m) = 1.727 (1 – 0.001i)

a) Free TE resonator

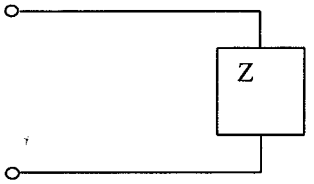

b) Mason's Model

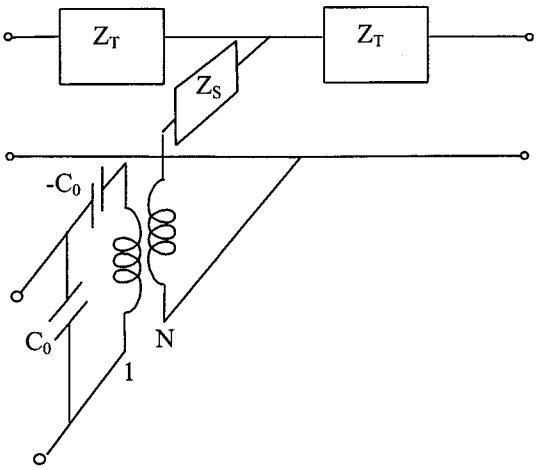

c) KLM Model

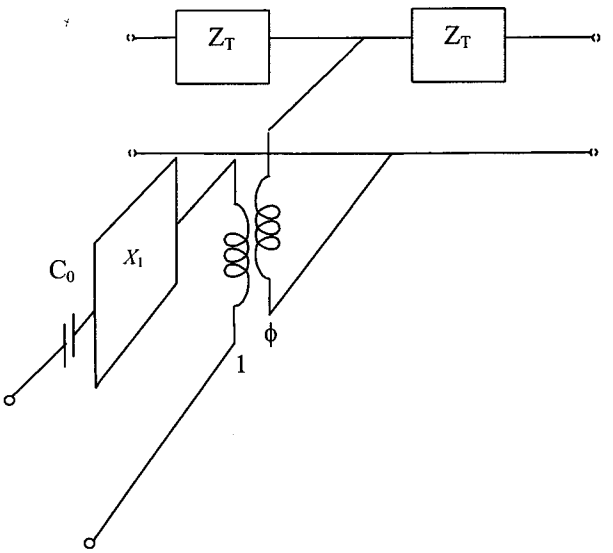

Figure 1. Sherrit et. al.

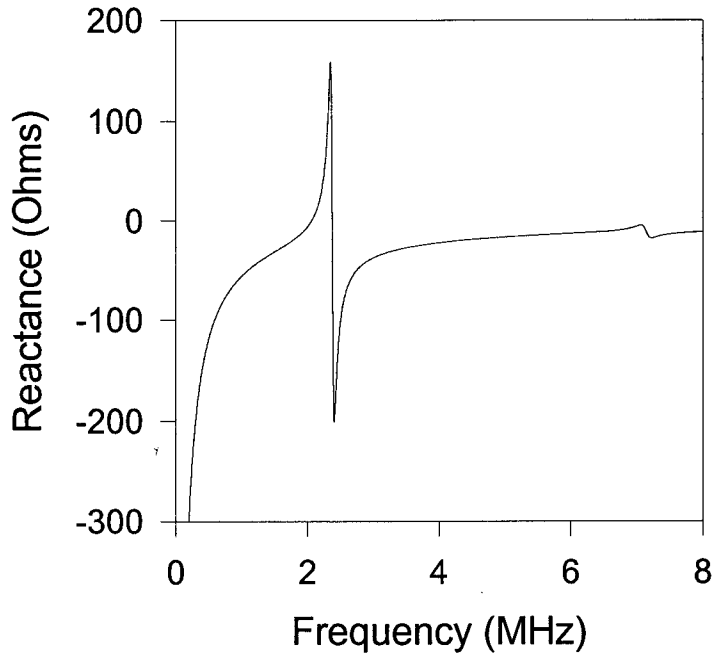

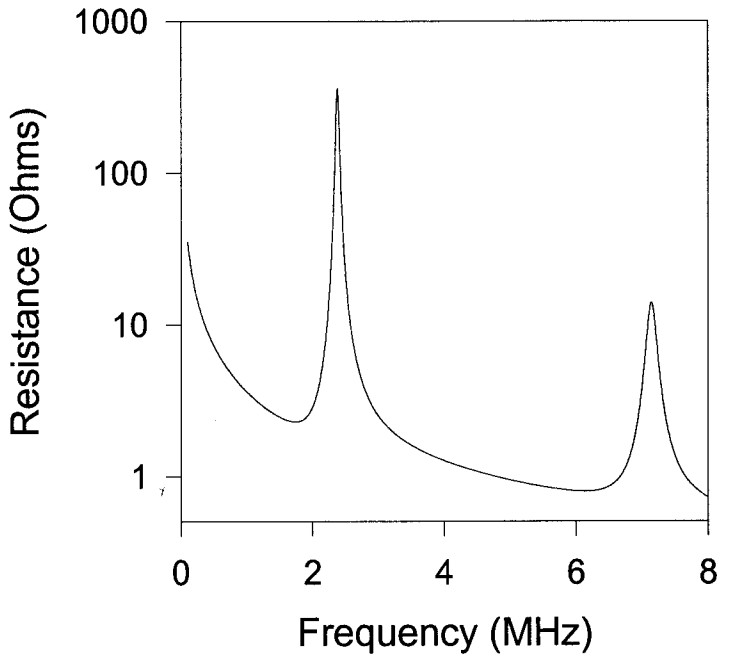

Figure 2 Sherrit et. al.

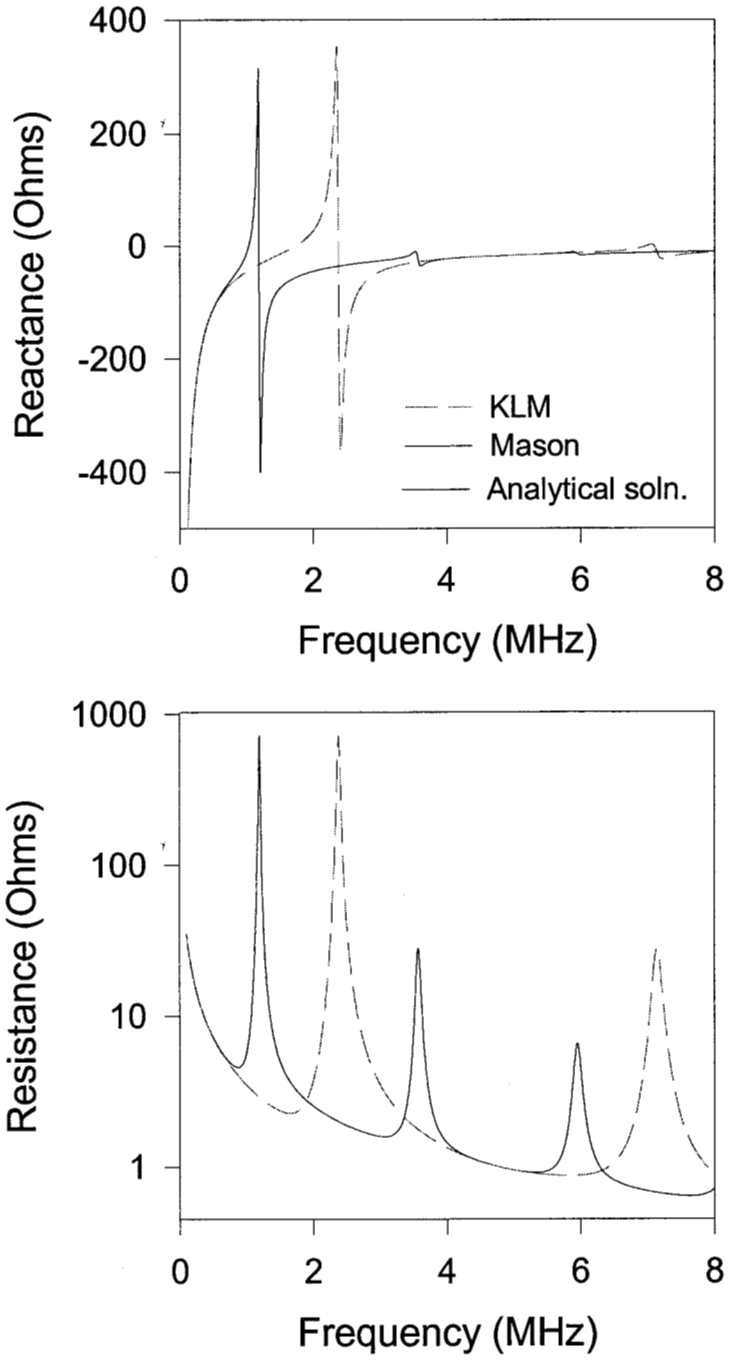

Figure 3. Sherrit et. al.

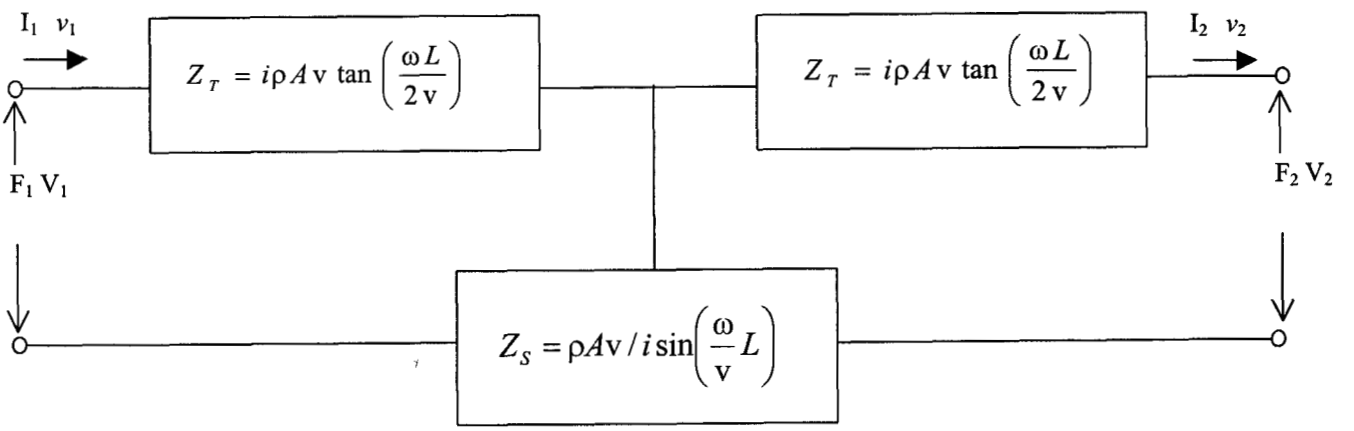

Figure 4. Sherrit et. al.

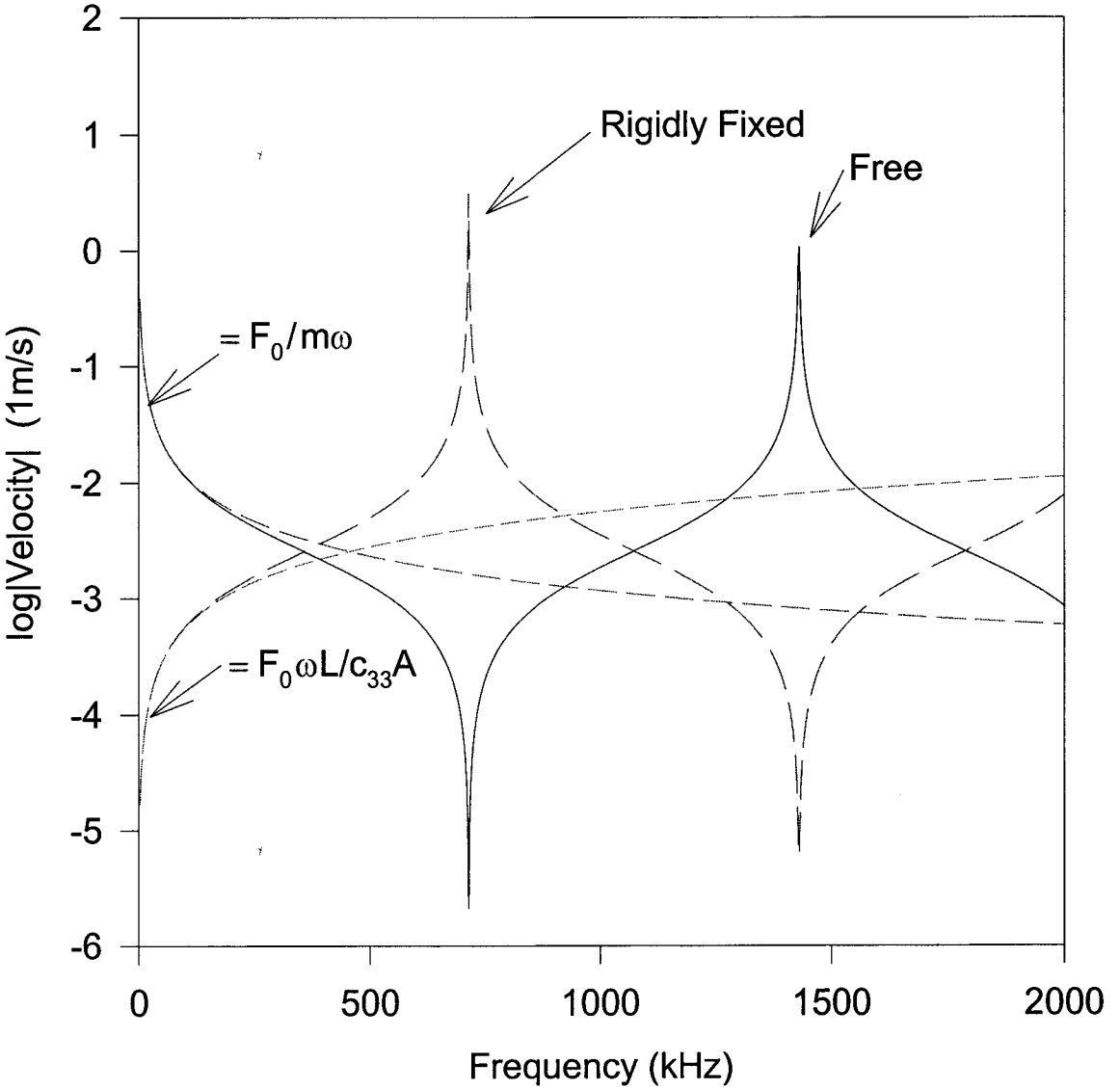

Figure 5. Sherrit et. al.

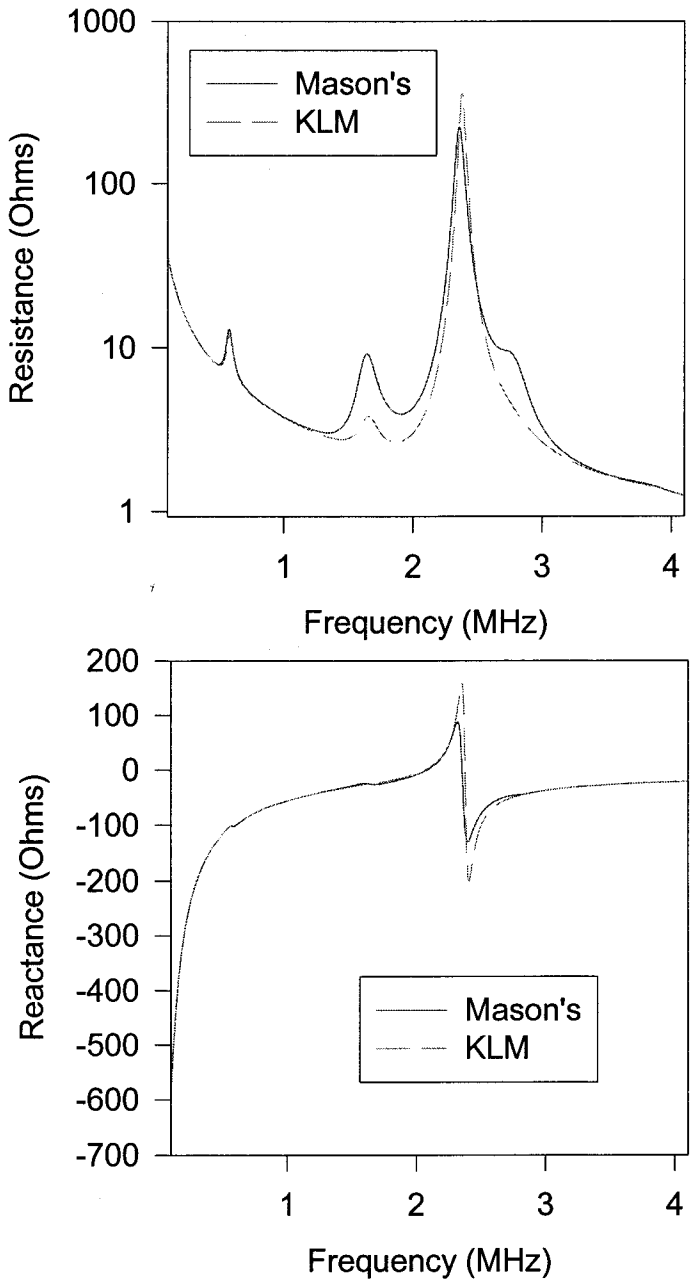

Figure 6. Sherrit et. al.

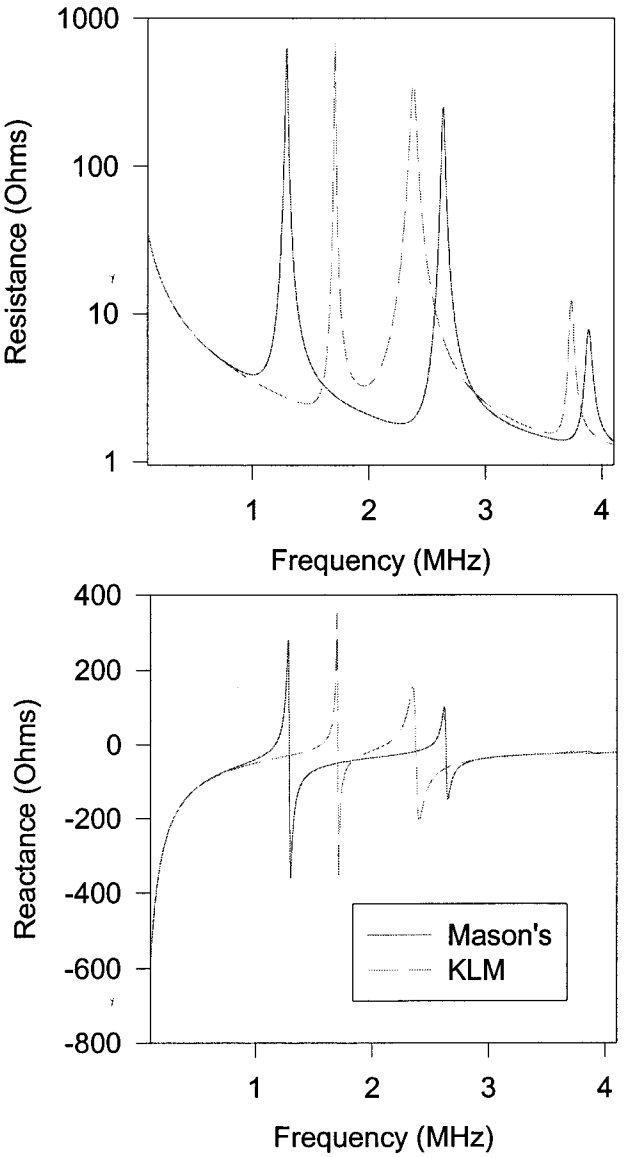

Figure 7. Sherrit et. al.

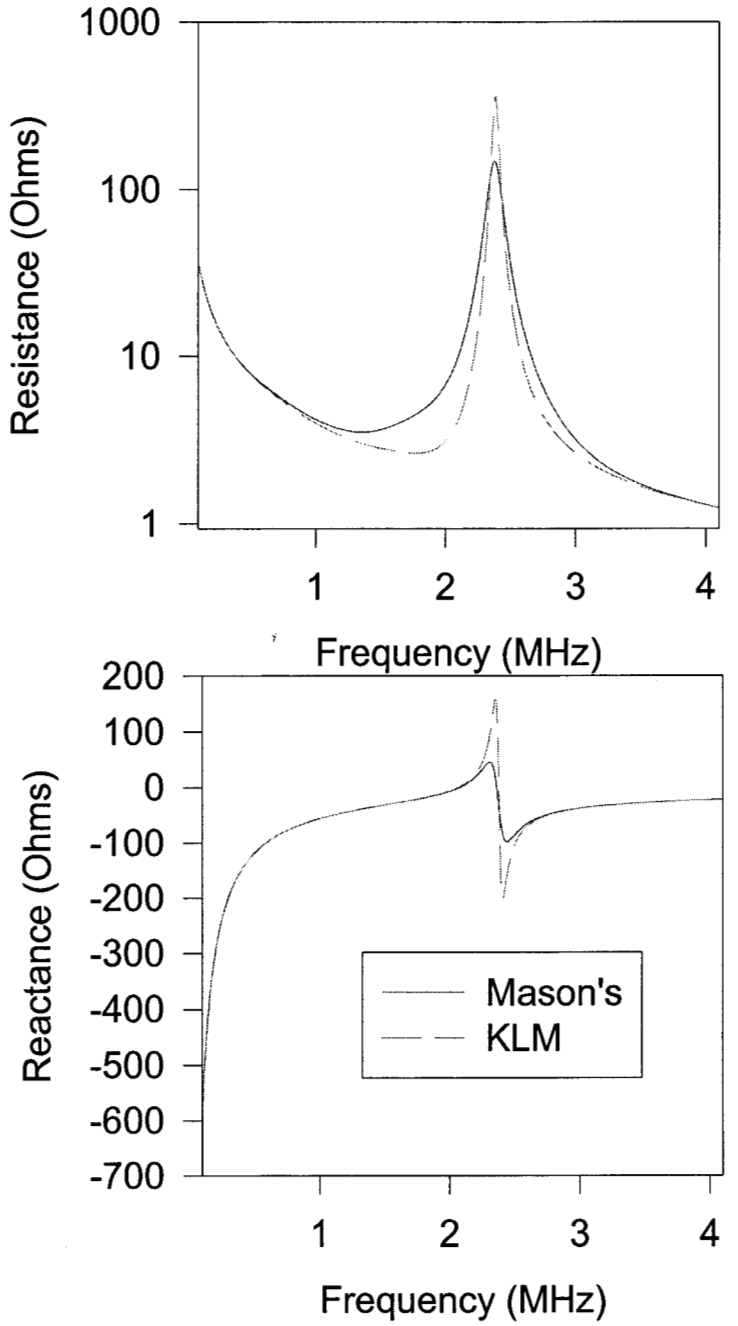

Figure 8 Sherrit et. al.

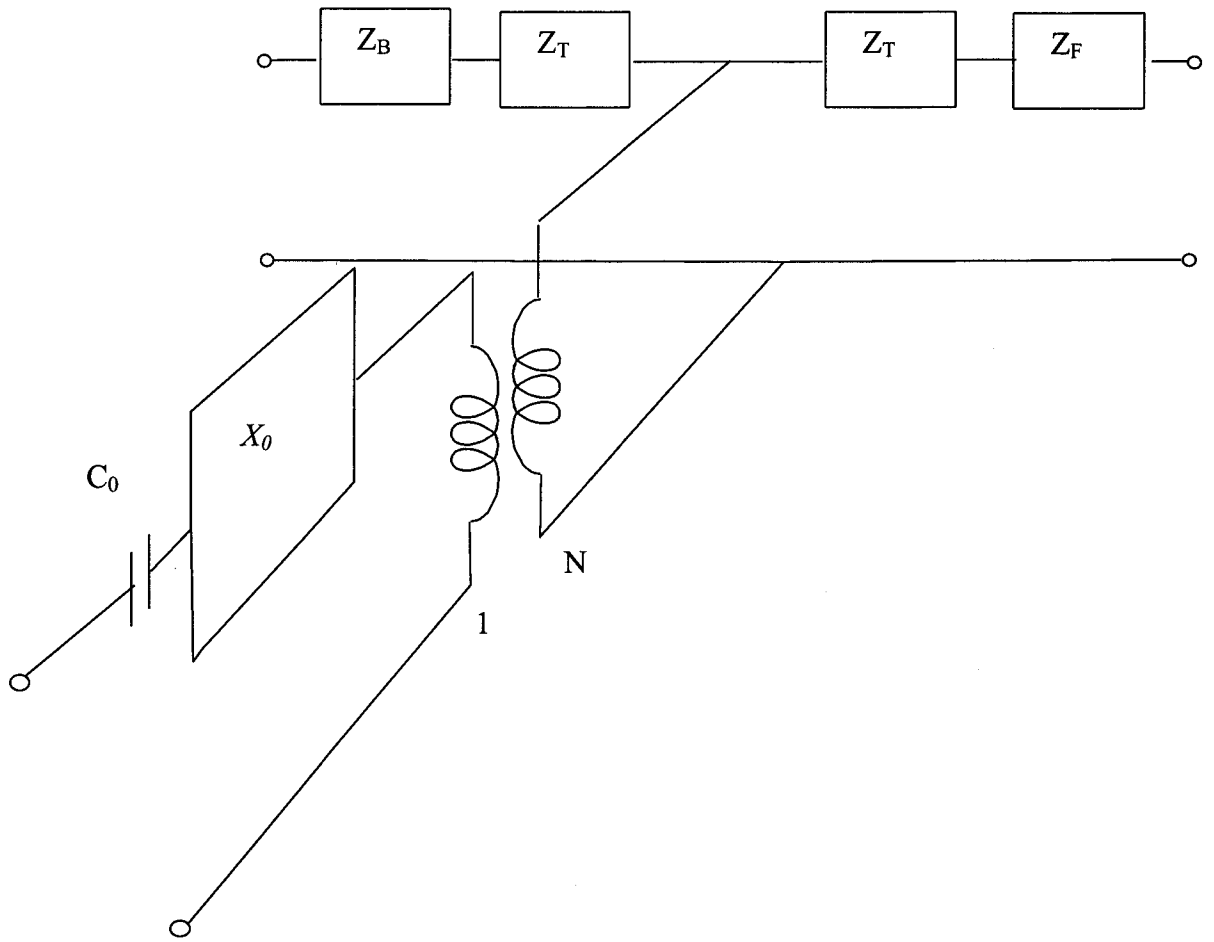

Figure 9. Sherrit et. al.